P1.12 MODELING CONVECTIVE WEATHER AVOIDANCE IN ENROUTE AIRSPACE*

Rich DeLaura†
Mike Robinson
Margo Pawlak
Jim Evans
Massachusetts Institute of Technology, Lincoln Laboratory
Lexington, MA 02420

It is generally agreed that effective management of convective weather in congested airspace requires decision support tools that translate the weather products and forecasts into forecasts of ATC impacts and then use those ATC impact forecasts to suggest air traffic management strategies. In future trajectory-based operations, it will be necessary to automatically generate flight trajectories through or around convective weather that pilots will find acceptable. A critical first step, needed in both today's air traffic management environment and in the highly automated systems of the future, is a validated model for airspace that pilots will seek to avoid.

At the 12th Conference on Aviation, Range and Aerospace Meteorology (Atlanta, 2006), we reported on an initial Convective Weather Avoidance Model (CWAM1) (DeLaura and Evans; 2006). The CWAM1 outputs are three dimensional deterministic and probabilistic weather avoidance fields (WAFs). CWAM1 used Corridor Integrated Weather System (CIWS) VIL and echo top fields and National Lightning Detection Network (NLDN) data to predict aircraft deviations and penetration. CWAM1 was developed using more than 500 aircraft-convective weather encounters in the Indianapolis Air Route Traffic Control Center (ZID ARTCC) airspace. CWAM1 gave the greatest weight to the difference between flight altitude and the 18 dbZ radar echo top with precipitation intensity playing a secondary role. The deviation prediction error rate in CWAM1 was approximately 25%.

This paper presents a new model (CWAM2), based on the analysis of trajectories from several ARTCCs [Indianapolis (ZID), Cleveland (ZOB) and Washington, DC (ZDC)] and an expanded set of meteorological deviation predictors. Additional weather factors that are considered include vertical storm structure (upper level reflectivity and the height of the VIL centroid derived from the NSSL 3D reflectivity mosaic), vertical and horizontal storm growth, the spatial variation in VIL and echo top fields and storm motion.

1. INTRODUCTION

Thunderstorms are a leading cause of delay in the US National Airspace System (NAS) (Comet), and significant convective weather is an almost daily occurrence in the highly congested northeastern US traffic corridor during the spring and summer (Robinson, et al, 2004). Aviation weather systems such as the Corridor Integrated Weather System (CIWS) Klingle-Wilson and Evans, 2005) and the National Convective Weather Forecast (NCWF) (Mueller, et al, 1999) provide weather products and forecasts that aid en route traffic managers in making tactical routing decisions in convective weather. However, the dynamic nature of convective weather and complexity of air traffic management in a rapidly changing weather environment makes it difficult to derive the full benefit of high quality convective weather products. In order to make the most effective use of convective weather information, traffic managers need automated decision support systems that integrate convective weather products into models of NAS operations to assist in developing and executing convective weather mitigation plans. Weather-aware decision support requires methods to determine regions of the airspace blocked by convective weather, estimate the impact of convective weather on scheduled traffic, provide re-routes that avoid convection and calculate the capacity that can be achieved using a particular weather avoidance strategy.

Several techniques have been proposed to estimate the capacity impact of convective weather (Post, et al, 2002), define routes that avoid convective weather (Prete and Joseph, 2004 and Winfield and Daniel, 2004) and calculate the capacity that is achievable along weather-avoiding routes (Mitchel, et al 2006). In all of these

*This work was sponsored by the National Aeronautics and Space Administration (NASA) under Air Force Contract FA8721-05-C-0002. Opinions, interpretations, conclusions, and recommendations are those of the authors and are not necessarily endorsed by the United States Government.
†*Corresponding author address*: Rich DeLaura, MIT Lincoln Laboratory, 244 Wood Street, Lexington, MA 02420-9185; e-mail: richd@ll.mit.edu

instances, the authors choose two dimensional spatial fields that are 'reasonable' but unvalidated representations of convective weather that must be avoided (VIP level 3 precipitation or cloud-to-ground lightning strikes) to illustrate their techniques. However, they stress that their techniques may be applied to *any* two-dimensional spatial field that defines airspace blockage. Two more recent studies (Martin, 2007 and Song et al, 2007) estimate sector capacities using WAFs from CWAM1 to define passable airspace.

There is a clear need to understand the nature of convective weather that pilots avoid in en route and terminal airspace. The FAA Aeronautical Information Manual suggests that pilots avoid thunderstorms characterized by "intense radar echo" in en route airspace by at least 20 nautical miles (40 km) (FAA, 2005). However, a study of pilot behavior in both terminal and en route airspace near Memphis, TN (Rhoda, et al, 2004) suggested that pilots fly over high reflectivity cells in en route airspace and penetrate lower cells whose reflectivity is less than Video Integrated Processor (VIP) level 3. A recent study [CWAM1] that developed a statistical model to predict pilot avoidance of convective weather in en route airspace found that the difference between flight altitude and the 18 dbZ radar echo top was the most accurate predictor of pilot deviation around convective weather, with precipitation intensity playing a secondary role. Using this model, one can calculate three dimensional weather avoidance fields (WAFs) that give the probability of pilot deviation due to convective weather at each pixel as a function of echo top height and precipitation intensity.

CWAM1 was based on a limited data set. Approximately 500 en route flight trajectories through the ZID ARTCC from five different days in 2003 with significant convective weather were analyzed. Avoidance predictors were derived from three weather data fields: VIL (measure of precipitation intensity), echo top height (storm height) and cloud-to-ground lightning strike counts from the National Lightning Detection Network (NLDN). Although a recent validation study (Chan, et al, 2007) found that the 80% probability of deviation regions from CWAM1 WAFs were generally accurate, observations of en route flight trajectories in convective weather also show that pilots readily penetrate regions characterized by both high echo tops and VIL intensity under certain circumstances (figure 1). This suggests that knowledge of echo tops and VIL alone are not always sufficient to determine if a region of airspace is passable.

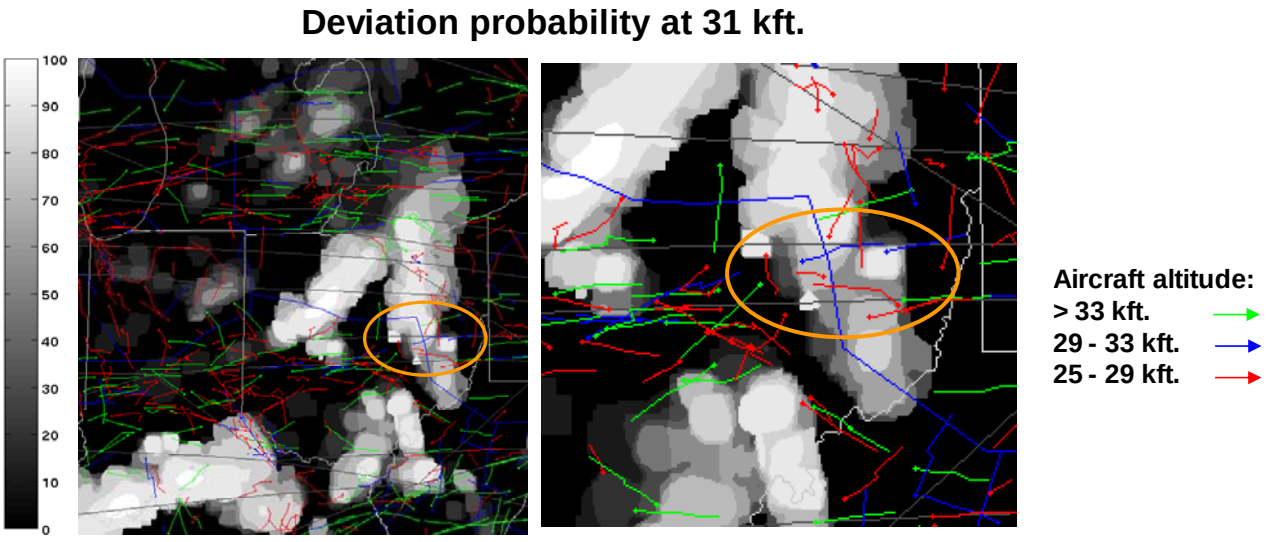

Figure 1. Illustration of traffic penetrating a CWAM1-derived weather avoidance field (WAF) region of high deviation probability, from 14 July, 2006.

In this paper, we present a revised model to predict pilot deviation around convective weather in en route airspace (CWAM2). Flight trajectory data were taken from the Enhanced Traffic Management System (ETMS); weather products were taken from CIWS and the National Severe Storms Laboratory (NSSL) national 3D reflectivity mosaic (Zhang, 2004). Three different geographical regions [the Indianapolis, Cleveland and Washington, DC ARTCCs – ZID, ZOB and ZDC, respectively] were studied (figure 2). Weather and trajectories from six different days in the summer of 2006 were examined to develop the deviation model. In addition, trajectories from four clear weather days were used to develop an operational definition of deviation. Table 1 summarizes the cases analyzed.

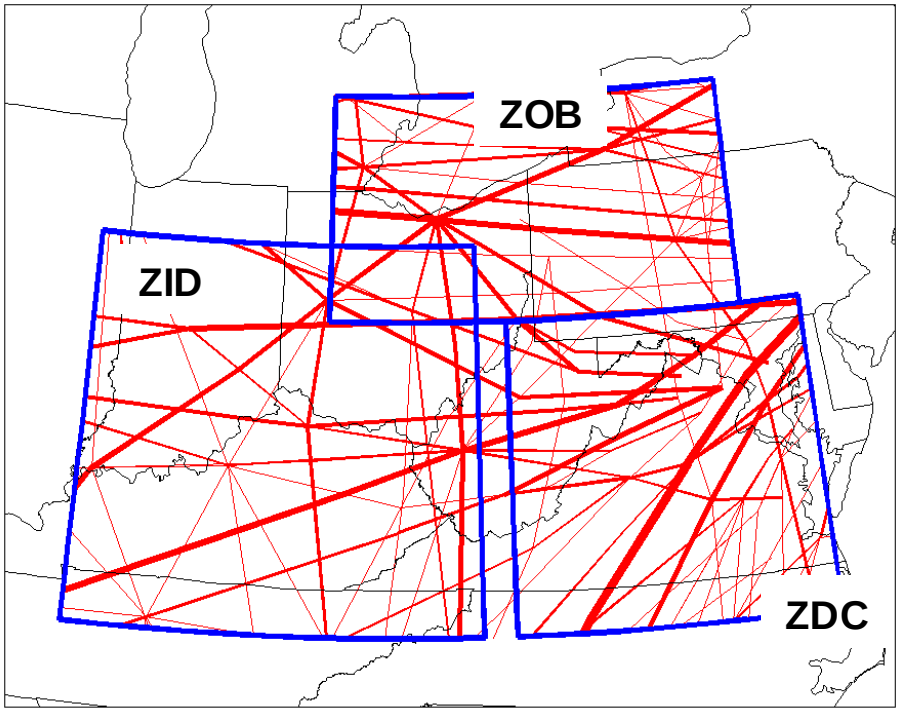

Figure 2. ARTCCs studied in CWAM2. Red lines are jet routes; thicknesses are proportional to peak traffic loads

Table 1. Summary of convective weather case days and where impacts occurred (all days in 2006).

Date	Start (GMT)	End (GMT)	ZDC impact	ZID impact	ZOB impact
01 June	1700	2400	X	X	X
19 June	0000	2400	X	X	X
23 June	0000	0800	X	X	
12 July	0800	1900		X	
14 July	1900	2400	X	X	X
22 September	1100	2400		X	

2. METHODS

ETMS provides the location (latitude, longitude, altimeter-based altitude) of each airborne flight in the NAS, updated every minute, and a list of the navigation fixes that the flight will pass thorough as it follows its filed flight plan. Only the trajectories of en route flights in the three analysis regions are considered, where en route flights are defined as those whose altitude is greater than 25000 feet at all times that the flights are within the region. Since ETMS does not provide a planned trajectory, one must be created. We use the technique developed for CWAM1, in which the ground speed and altitude of the actual flight trajectory are applied to the path that connects the filed flight plan navigation fixes. Altimeter altitudes were converted to geometric height above sea level using sounding data and the altimeter equation (Wallace and Peter, 1977), so that they could be compared to echo top heights. Both planned and actual trajectories are interpolated to 10 second intervals.

Weather encounters along planned flight trajectories (portions of a planned trajectory that pass through *either* VIL level 2 or greater *or* echo tops of 25000 feet or greater for at least 2 minutes) are identified and automatically classified as deviations or non-deviations. A weather encounter is classified as a deviation if the RMS horizontal distance between the actual and planned trajectories for the duration of the encounter exceeds the deviation threshold of jet routes in the region through which the trajectory passes. Weather encounter classifications from the automated algorithm were reviewed by an analyst and misclassified encounters were removed from the analysis. Figure 3 illustrates two weather encounters, a deviation and non-deviation. Approximately 800 weather encounters – almost all encounters where the pilot deviated from the planned trajectory for non-weather reasons such as airborne holding or corner-cutting - were edited out of the original set of approximately 2760 encounters due to classification errors. Table 2 summarizes the encounters analyzed. Other reasons for editing encounters were slowdowns due to downstream volume congestion, 'serial' encounters (second or third encounters that followed an initial deviation) or instances where pilot intent was impossible to ascertain from the trajectory data. Encounters were also eliminated from the analysis if any of the weather predictors was not available for any reason. Figure 4 illustrates common classification errors from the automated deviation detection algorithm.

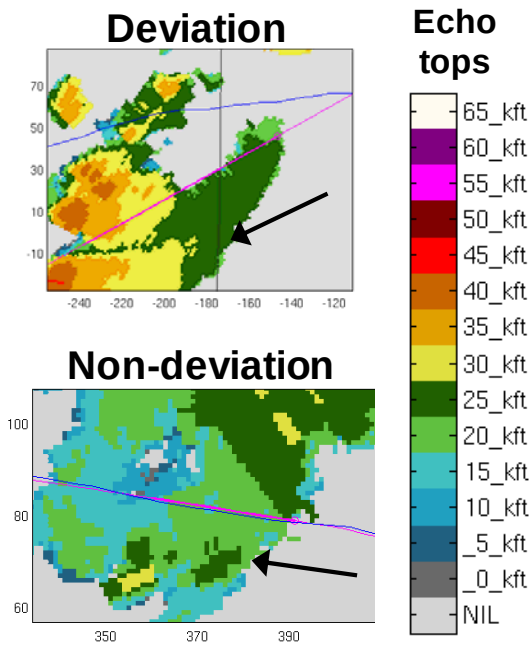

*Figure 3. Flight trajectories (**planned** and **actual**) overlaid on observed echo tops. Top trajectory is a weather-related deviation; the flight altitude is 34 kft. Bottom is a non-deviation; flight altitude starts at 39 kft and descends to 34 kft. Black arrow shows direction of travel.*

Table 2. Weather encounters and deviation classifications.

	Total	Deviations	Non-deviations
ZDC	432	238	194
ZID	521	198	323
ZOB	1002	232	770
Total	1955	668	1287

The deviation threshold is defined by analyzing planned and actual trajectories from four convection-free days. First, trajectory elongation (the ratio between the actual and planned trajectory lengths) for each flight is calculated. Flights with trajectory elongation << 1 (short cuts) and trajectory elongation >> 1 (non-weather related operational deviations such as vectoring to avoid congestion) are eliminated from the analysis. The remaining flights, with trajectory elongation near unity, are assumed to be following the planned path. For each of these flights, the RMS horizontal deviation distance is calculated and the deviation threshold is defined as the 90th percentile of these RMS distances. Note that the

deviation threshold varies from one geographical region to the next, since it is likely to be related to the route structure and complexity of traffic flows in the region. The deviation threshold was 10 km. in ZID, 9 km. in ZOB and 7 km. in ZID.

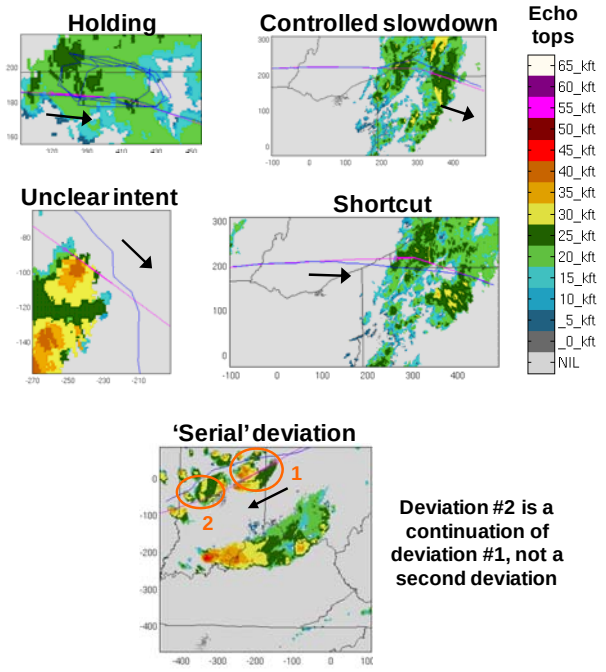

*Figure 4. Examples of deviation detection errors in the automated weather-related deviation detection algorithm. Flight trajectories (**planned** and **actual**) overlaid on observed echo tops. Black arrow shows direction of travel.*

This study considers a much larger set of weather characteristics as possible predictors of weather avoidance than the one used in CWAM1. Additional weather products provide information about storm evolution, vertical and horizontal structure and weather type, as well as precipitation intensity and storm height. CIWS weather products used in the study include VIL (precipitation intensity, see Crowe and Miller, 1999), echo tops (storm height), horizontal growth and decay, time derivative of echo tops and weather type (convective / non-convective). Upper level radar reflectivity and the height of VIL centroid, intended to capture information about the vertical structure of the storm, are calculated from the national NSSL 3D reflectivity mosaic. Note that CIWS VIL is expressed as an 'interest level', ranging between 0 and 254, which is proportional to the log of VIL (kg / m^2) (Troxel and Engholm, 1990). The interest level is mapped to an equivalent VIP value, with an interest level of 13 corresponding to VIP level 1, 73 to VIP level 2, 133 to VIP level 3, 159 to VIP level 4, 181 to VIP level 5 and 216 to VIP level 6.Note that CIWS VIL is expressed on a scale ranging from 0 to 254, with a value of 13 corresponding to VIP level 1, 73 to VIP level 2, 133 to VIP level 3, 159 to VIP level 4, 181 to VIP level 5 and 216 to VIP level 6.

Weather characteristic fields used as deviation predictors are derived from ***observed*** weather products (not forecasts) by using three different sized spatial filters (4x4, 16x16 and 60x60 km) to calculate statistics (median, percent area coverage, etc.) at each pixel in the field. For example, several weather characteristic fields are calculated from the VIL input: 90th percentile, median and 10th percentile VIL intensity, intensity variation (90th-10th percentile) at all spatial scales and percent coverage of VIP level 3, level 4 and level 5 pixels (16x16 and 60x60 km scales). Approximately 30 different weather characteristic fields were calculated, from which over 100 deviation predictors were derived; figure 5 illustrates several examples.

A value for each weather characteristic was assigned to every point of the planned and actual flight trajectories using the nearest neighbor from the weather characteristic field grid. For each weather encounter, the deviation predictors were derived from the extracted characteristic values. For example, values were extracted along the planned trajectory from the 90th percentile VIL, 60x60 km weather characteristic field; the maximum of these values is chosen as the 'large scale maximum VIL intensity' predictor (figure 6). In this way, predictors are generated that capture the scale, intensity and variation of the convective weather features encountered along the trajectory. Planned trajectories were also offset in time (+/- 15 and 30 minutes) and run through VIL and echo top fields in an effort to generate predictors that capture storm motion (i.e., to identify planned trajectories that pass in front of or behind moving storms). Table 3 summarizes the complete set of predictors considered.

The deviation classifications and predictor set for all weather encounters were input to a Gaussian classification algorithm (Lippmann et al, 1993 and Duda et al, 2001), as in the CWAM1 study. The classifier identifies the predictor set that minimizes the *total* encounter classification error (both deviation and non-deviation) and defines the decision boundary surface in multi-dimensional predictor space that separates deviations from non-deviations. Once this set of 'best' predictors was identified, a series of modeling experiments was carried out with several subsets of the best predictors to determine the

impact of different predictors on the classification error and to see if it was possible to reduce the number of predictors in the model without significantly increasing the error.

The deviation probability model was derived from the observed deviation statistics, partitioned into histogram bins defined for the best predictors. The deviation histograms were smoothed and extrapolated to define the probability of deviation as a function of the selected predictor set.

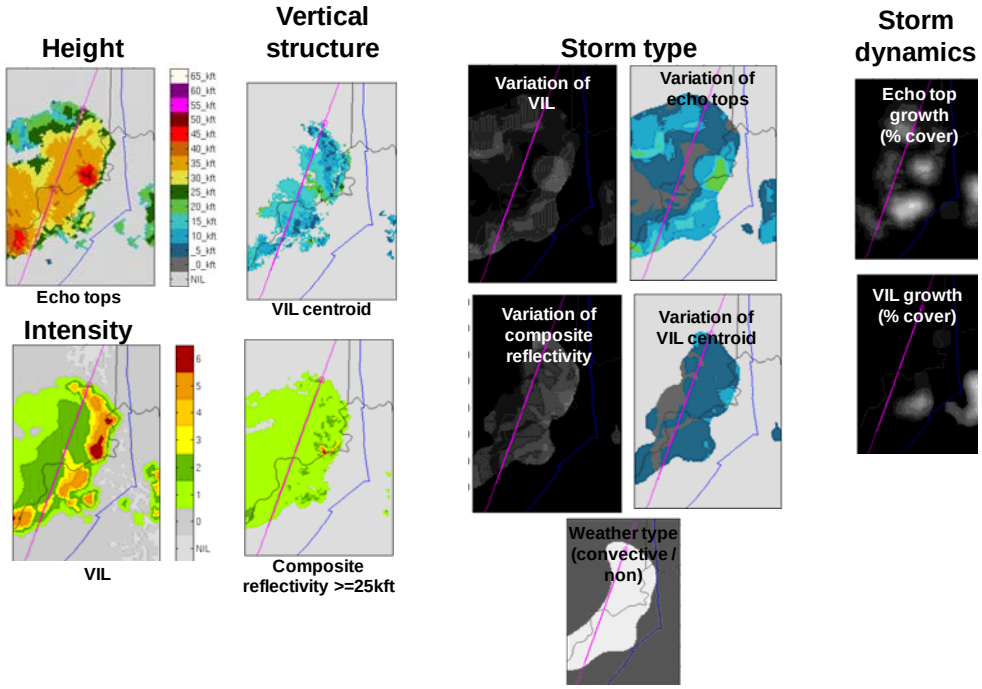

*Figure 5. Illustrations of weather products from which deviation predictors were derived. Flight trajectories (**planned** and **actual**) are overlaid.*

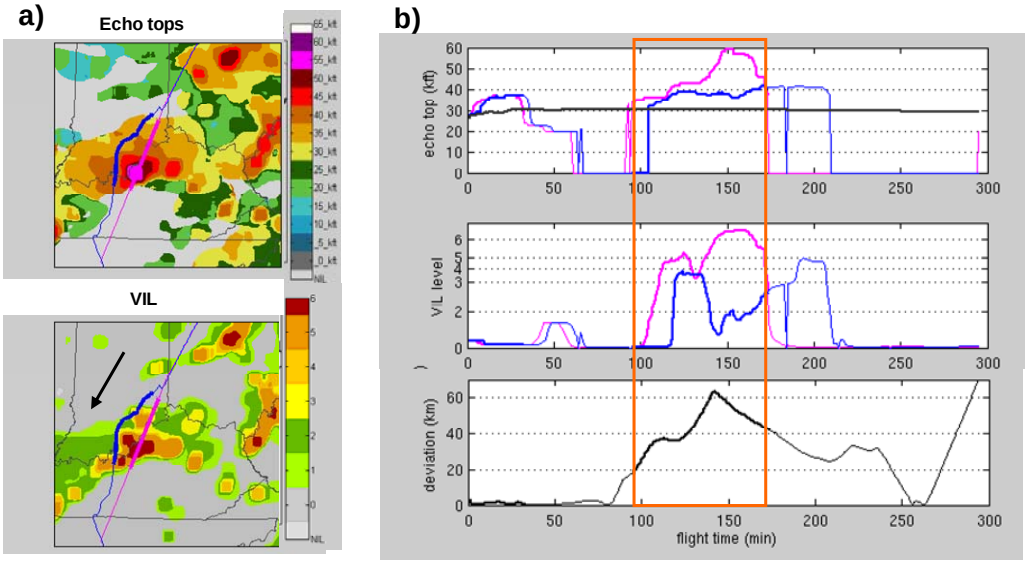

*Figure 6. Extracting weather data along **planned** and **actual** trajectories. Figure (a) shows echo tops (top) and VIL (bottom), 90th percentile values from the 4 x 4 km spatial filter. The black arrow shows the direction of flights. This encounter was flagged as a deviation. Figure (b) shows the echo top (top) and VIL (middle) data extracted along the trajectories; the period of the weather encounter is outlined by the orange box. Bottom plot shows the deviation distance.*

Table 3. Summary of deviation predictors.

Weather	**Scale**		
	4 x 4 km	**16 x 16 km**	**60 x 60 km**
VIL Intensity			
90^{th}, 50^{th},10^{th} percentile	X	X	X
% cover level 3, 4, 5		X	X
Echo top height			
90^{th}, 50^{th},10^{th} percentile	X	X	X
% cover 30,40,50 kft		X	X
Trends			
% cover VIL growth		X	X
% cover echo top growth		X	X
Vertical structure			
VIL centroid 90^{th}, 50^{th}, 10^{th} percentile	X	X	X
Composite reflectivity (>=25 kft.) 90^{th}, 50^{th}, 10^{th} percentile	X	X	X
Weather type			
CIWS 'convective'	X	X	
VIL variation (90^{th}-10^{th} percentile)	X	X	X
Echo top variation (90^{th}-10^{th} percentile)	X	X	X
Flight relative			
Flight altitude – echo top	X	X	X
Flight altitude – VIL centroid	X	X	X
Storm motion			
Echo tops 90^{th}, 50^{th}, 10^{th} percentile, +/-15, 30 minutes		X	
VIL 90^{th}, 50^{th}, 10^{th} percentile, +/-15, 30 minutes		X	

Modeling experiments were performed on the complete set of weather encounters from all three ARTCCs and on the set of weather encounters from each individual ARTCC to determine if there were significant differences between weather avoidance in different ARTCCs. Modeling experiments were also run using the CWAM1 predictors and predictor sets that excluded echo top information.

3. RESULTS

There are two types of model classification error: deviations may be misclassified as non-deviations ('missed detections') or vice-versa ('false alarms'). Two models with similar overall error rates [(missed detections + false alarms) / (total encounters)] may have very different missed detection and false alarm rates. One cannot determine objectively which model is 'best', without an explicit cost weighting assigned to each error type. In this analysis, we present overall error rates, missed detection and false alarm rates.

Figure 7 summarizes the results. Five predictors were found to have skill in classifying encounters: the difference between flight altitude and 90^{th} percentile echo top height from the 16 x 16 km spatial filter (DZ_ETOP_16); variation of VIL (90^{th} – 10^{th} percentile) from the 60 x 60 km spatial filter (VILVAR_60); percent coverage of echo top >= 30 kft. (16 x 16 km, ETOP_C030_16); 90^{th} percentile echo top height (16 x 16 km, ETOP_P090_16) and 90^{th} percentile composite reflectivity from 25 kft and above (16 x 16 km, COMPREFL_25_P090_16). The figure shows the overall error rate (blue), false alarm rate (green) and missed detection rate (red) for all regions (square), ZDC (triangle), ZID (plus sign) and ZOB (circle). Errors are plotted for the best 5, 4, 3 and 2 predictor models from CWAM2, the best predictor model without echo top information (VILVAR_60, COMPREFL_25_P090_16 and 90^{th} percentile VIL, 60 x 60 km, VIL_P090_60) and the CWAM1 predictor model (DZ_ETOP_16 and percent coverage with VIL >= VIP level 3, 60 x 60 km spatial filter, VIL_C003_60).

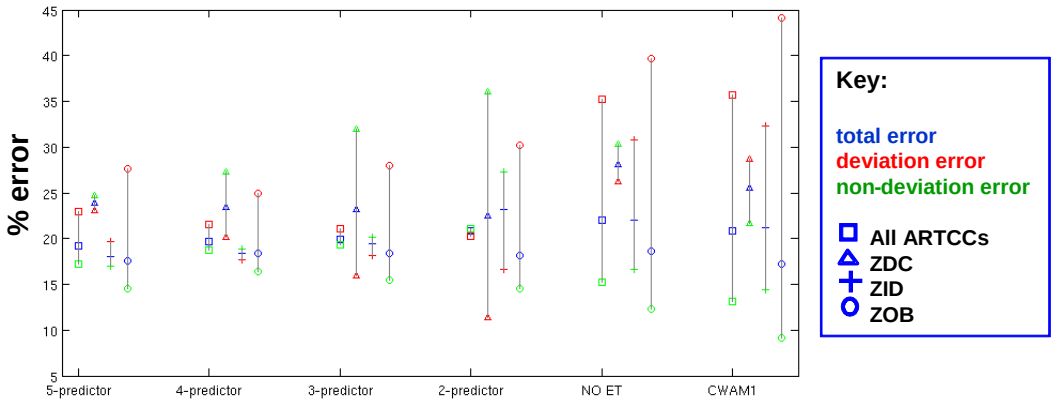

5 predictor	**DZ_ETOP_16, ETOP_C030_16, VILVAR_60, ETOP_P090_16, COMPREFL_25_P090_16**
4 predictor	**DZ_ETOP_16, ETOP_C030_16, VILVAR_60, ETOP_P090_16**
3 predictor	**DZ_ETOP_16, ETOP_C030_16, VILVAR_60**
2 predictor	**DZ_ETOP_16, ETOP_C030_16**
NOET (no echo tops)	**VILVAR_60, COMPREFL_25_P090_16, VIL_P090_60**
CWAM1	**DZ_ETOP_16, VIL_C003_60**

Figure 7. Summary of classification errors for deviation prediction models. Predictors are defined in the text.

Figure 7. Summary of classification errors for deviation prediction models. Predictors are defined in the text.

Several things are evident in the results. The overall classification error rates for all models (no echo tops and CWAM1 included) are very similar, at least when encounters from all ARTCCs are considered together (square symbols on the error plot). There are significant differences, however, in the spread between false alarm and missed detection rates and in the classification error rates for individual ARTCCs. Both the CWAM2 no-echo-top model and the CWAM1 model have larger error spreads than the CWAM2 models with echo top predictors; differences between false alarm and missed detection rates are greater, as are the differences between error rates in different ARTCCs.

The five predictor model provides only marginal improvement in the overall error rate and actually increases the difference between missed detection and false alarm error rates compared to the four predictor model; apparently, the fifth predictor (COMPREFL_25_P090_16) adds little benefit. Reducing the number of predictors from four to three to two does not significantly increase the overall error rate. However, the difference between missed detection and false alarm rates does increase as the number of predictors decreases, as does the variation in error between ARTCCs. The CWAM2 models appear to work best in ZID, with lower overall errors and a small spread between missed detection and false alarm rates. Interestingly, false alarm rates were greater than missed detections in ZDC, while the situation was reversed in ZOB. This may be due to operational differences in the two ARTCCs; for instance, ZOB may be more able to accommodate deviation than ZDC, making pilots more willing to ask for deviations around marginal weather in ZOB. The differences may also be due to the relatively small number of weather encounters in each individual ARTCC. In any event, further research is required to understand the observed differences.

Figure 8 shows the results for the two predictor (DZ_ETOP_16, ETOP_C030_16) model.

Figure 8a is a scatterplot of all encounters, with the boundary between deviation and non-deviation in the background and the encounters erroneously classified by the model in gray. Figure 8b is a 2D histogram showing the observed deviation probabilities as a function of the two predictors. Figure 8c is a 2D histogram of the modeled probability of deviation derived from the observed probabilities.

a) Decision model

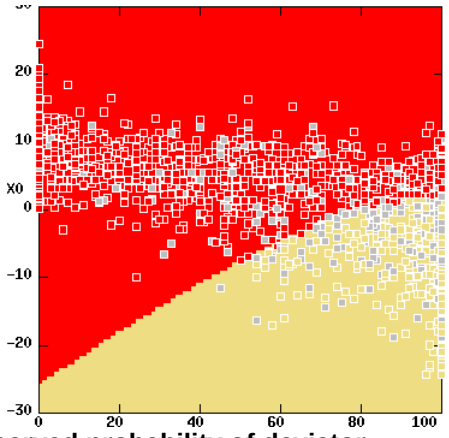

b) Observed probability of deviator

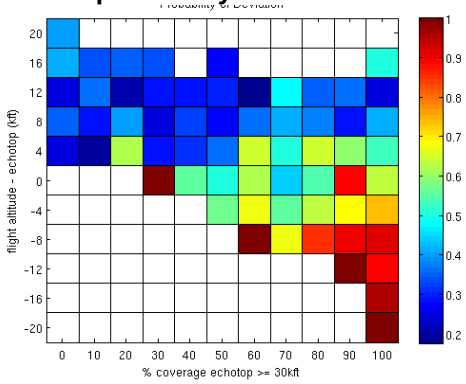

c) Modeled probability of deviation

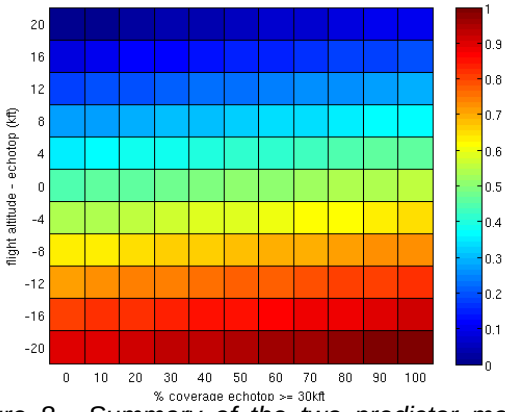

Figure 8. Summary of the two predictor model. Figure (a) shows a scatter plot of all encounters, with the boundary between deviations and non-deviations. X-axis is % coverage with echo top >= 30 kft. (16 x 16 km); Y-axis is flight altitude – 90th percentile echo top (16 x 16 km). Gray filled squares indicate encounters that were misclassified by the model; note the cluster of errors where flight altitude was roughly equal to or slightly less than echo top height. Figure (b) shows the observed probability of deviation, with the same X and Y axes as figure (a). White squares indicate histogram bins with no data. Figure (c) shows the modeled 2D probability function derived from the observed probabilities in figure (b).

The classification errors are clustered around encounters with flight altitudes roughly comparable to or slightly less than the echo top height (and where the observed probability of deviation is roughly in the range of .4 to .6). The inability of the CWAM2 model to differentiate between echo tops at flight altitude that pilots appear to view as benign and those that they wish to avoid may be due to any one of a number of factors. Knowledge of upper level winds may be needed to differentiate hazardous downwind thunderstorm anvils from relatively benign regions of high-topped stratiform rain, whose echo top and VIL signatures appear similar. Figure 9 illustrates an example of each, showing photos taken from during a flight mission on 30 August, 2007 and corresponding VIL and echo top fields.

Other factors that were not considered in the CWAM2 study may help explain observed pilot deviation decisions. These include weather information that cannot be easily derived from ground or satellite-based weather sensors (cockpit visuals, for example) or that are related to pilot training, aviation company policies or the pilot's risk tolerance. Figure 10 illustrates two weather encounters, 10 minutes apart, flying in the same direction on the same en route airway in eastern ZOB. The flights encounter virtually identical weather and their altitudes are roughly the same, yet the first flight deviates widely around the weather and the second penetrates without any discernable alteration of course. The CWAM2 predictor set did not include anything that might have helped differentiate between these two pilots' behavior.

Finally, the Gaussian classifier models the distributions of deviations and non-deviations about the input predictors as Gaussians. While many of the predictors studied were well suited to Gaussian modeling, some were not. A poor fit of these distributions will result in classification errors. Another classification scheme may be

more appropriate. We tried to apply a k-nearest-neighbor scheme (Lippman et al, 1993 and Duda et al, 2001), with k=3 and k=5, but the results were significantly worse that the those obtained using the Gaussian classifier.

The decision space for the three and four predictor models is difficult to visualize and the analysis of these models has not yet been completed. As the number of predictors increases, the dimensionality of the deviation probability function also increases and a larger set of encounter statistics is needed to fit the deviation probability function. A larger encounter database will be needed to estimate a deviation probability function of three or four input predictors.

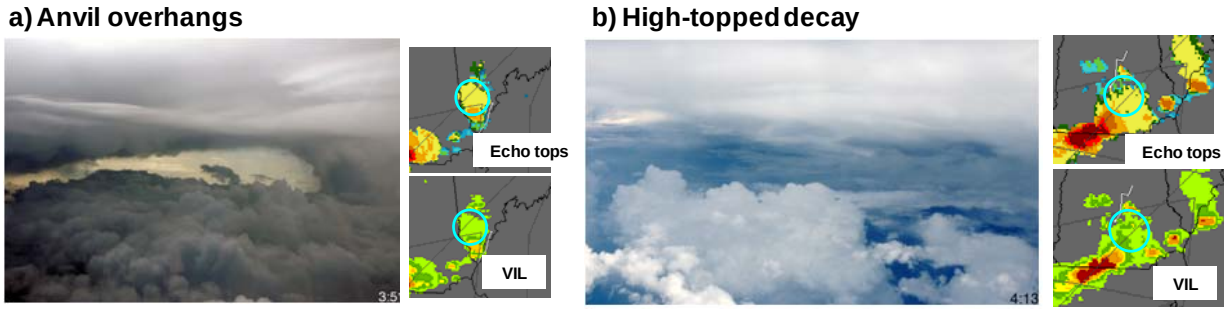

Figure 9. Photographs showing a thunderstorm anvil overhang (a), taken from 28 kft., and a region of high echo top decay behind the leading edge of a storm (b), taken from 35 kft. Pilots tend to avoid anvils, where convective activity is vigorous and growing and where flights will experience significant turbulence. Pilots are more likely to penetrate or fly over regions of high-topped decay, where convective activity is weak and turbulence is minimal.

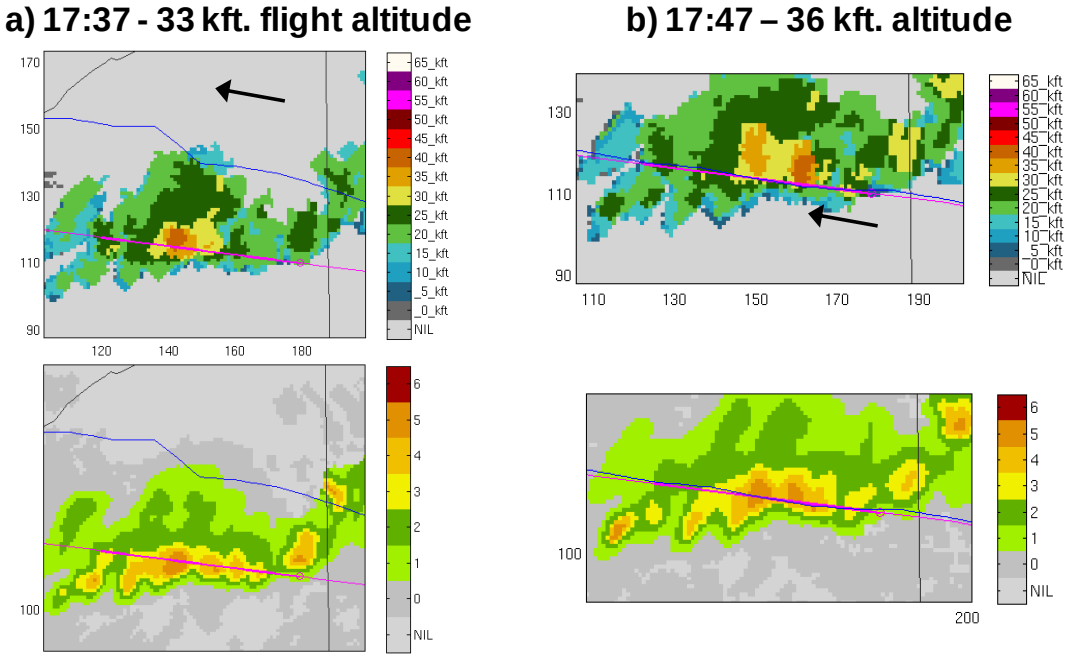

*Figure 10. Flight at 33 kft. altitude deviates around 35-40 kft cell at 17:37 (a). Flight at 36 kft. flies straight through the same cell at 17:47 (b) Flight trajectories (**planned** and **actual**) are overlaid on*

observed echo tops(to) and VIL (bottom). Black arrows indicate direction of travel. Example is taken from 01 June, 2006.

4. CONCLUSIONS

This study (CWAM2) extends the initial exploratory convective weather avoidance modeling study (CWAM1) reported in 2006. It presents a statistical model to predict pilot deviation around convective weather in en route airspace. Nearly 2000 weather encounters from three ARTCCs (ZDC, ZID and ZOB) on six different days in 2006 were analyzed. Deviations were identified using flight track data from ETMS and more than 100 deviation predictors were derived from CIWS and NSSL weather products.

CWAM2 confirmed the finding of the original study that the difference between flight altitude and echo top height is the single best predictor of pilot deviation around convective weather in en route airspace. Only one of the five best predictors of deviation identified by a Gaussian classifier algorithm was not related to echo top height (the difference between 90th and 10th percentile of the VIL, where percentiles were calculated over a 60 x 60 km region). Prediction errors were greatest for trajectories whose flight altitude was near or slightly below the echo top height and the differentiation between 'benign' echo tops and those that pilot avoid remains the major challenge in convective weather avoidance modeling.

It may be surprising that measures of precipitation intensity (maximum VIL, composite reflectivity, etc.) do not provide additional deviation prediction skill beyond what is available in the echo top fields. However, for flights at en route cruising altitudes, regions of heavy but low-topped precipitation are readily over flown. Where heavy precipitation is due to vigorous convective activity, both high VIL and echo tops are present. Echo top heights alone can explain observed pilot behavior in both circumstances. Note that in other phases of flight – departures and arrivals in the terminal area or transition from terminal area to en route airspace – aircraft are traversing different altitudes and pilots have different concerns that may be more closely related to precipitation intensity measured by VIL.

Going forward, several areas of continued research are needed:

1) Development of an improved deviation detection algorithm to enable the creation of large scale trajectory and deviation databases for modeling and validation studies
2) Consideration of important weather data such as upper level winds and satellite data as possible deviation predictors
3) Review of existing data such as echo top trends and storm motion data to ensure that predictors based on these products were well-chosen
4) Consideration of human factors, such as cockpit information, pilot training, company policies, etc. as possible deviation predictors.

It is also necessary to extend the research into terminal area and transitional airspace to develop convective weather avoidance models for ascending and descending aircraft. Finally, research is needed to determine how to use weather avoidance fields based on convective weather avoidance models in airspace capacity algorithms and operational decision support tools.

5. ACKNOWLEDGMENTS

The authors wish to thank Brad Crowe, Richard Ferris, Todd Lardy, Kenneth Bonk and Thomas Burbine at Lincoln Labs for those fabulous thunderstorm photos. Brad directed the flight missions, Richard monitored the real time weather feeds and steered the flights from the ground, Todd and Kenneth piloted the aircraft and Thomas took the photographs.

6. REFERENCES

Chan, William, Mohamad Refai, Rich DeLaura: "An Approach to Verify a Model for Translating Convective Weather Information into Air Traffic Management Impact", 7th AIAA-ATIO Conference, Belfast, Northern Ireland, September, 2007.

Cooperative Program for Operational Meteorology, Education and Training (COMET®): http://meted.ucar.edu/nas/index.htm.

Crowe, B. A. and D. W. Miller: "The Benefits of Using NEXRAD Vertically Integrated Liquid Water as an Aviation Weather Product", 8th Conference on Aviation, Range and Aerospace Meteorology. American Meteorological Society, Dallas, TX, 1999.

DeLaura, Rich, and James Evans: “An exploratory study of Modeling Enroute Pilot Convective Storm Flight Deviation Behavior”, 12th Conference on Aviation, Range and Aerospace Meteorology, American Meteorological Society, Atlanta, GA, January, 2006.

Duda, Richard O., Peter E. Hart, David G. Stork: Pattern Classification, Second Edition, John Wiley & Sons, Inc., 2001, pp 20-63.

FAA Aeronautical Information Manual, February, 2005.

Klingle-Wilson, D., J. Evans: “Description of the Corridor Integrated Weather System (CIWS) Weather Products”, MIT Lincoln Laboratory Project Report ATC-317, August, 2005.

Lippmann, R.P., L. Kukolich and E. Singer: “LNKnet Neural Network Machine Learning, and Statistical Software for Pattern Classification”, The Lincoln Laboratory Journal, Vol. 6, No. 2, 1993.

Martin, Brian D.: “Model Estimates of Traffic Reduction in Storm Impacted En Route Airspace”, AIAA Aviation Technology, Integration and Operations Conference, Belfast, Ireland, September, 2007.

Mitchell, Joseph S. B., Valentin Polishchuk, Jimmy Krozel: “Airspace Throughput Analysis Considering Stochastic Weather”, AIAA Guidance, Navigation and Control Conference, Keystone, CO, August, 2006.

Mueller, Cynthia K, Cynthia B. Fidalgo, Donald W. McCann, Dan Meganhardt, Nancy Rehak, Tom Carty: “National Convective Weather Forecast Product”, 8th Conference on Aviation, Range, and Aerospace Meteorology, Dallas, TX, January, 1999.

Rhoda, D.A., E.A. Kocab, M.L. Pawlak: “Aircraft encounters with convective weather in en route vs. terminal airspace above Memphis, Tennessee”, 10th Conference on Aviation, Range and Aerospace Meteorology, American Meteorological Society, Portland, OR, October, 2004.

Robinson, M., J. Evans, B. Crowe, D. Klingle-Wilson, S. Allan, 2004: “Corridor Integrated Weather System Operational Benefits 2002-2003: Initial Estimates of Convective Weather Delay Reduction”, MIT Lincoln Laboratory Project Report ATC-313, April, 2004.

Post, Joseph, James Bonn, Mike Bennett, Dan Howell, Dave Knorr: “The Use of Flight Track and Convective Weather Densities for National Airspace System Efficiency Analysis”, IEEE Digital Aviation Systems Conference, October, 2002.

Prete, Jopseph, Joseph S. B. Mitchell: “Safe Routing of Multiple Aircraft Flows in the Presence of Time-Varying Weather Data”, AIAA Guidance, Navigation and Control Conference, Providence, RI, August, 2004.

Song, Lixia, Craig Wanke, Daniel P. Greenbaum, David A. Callner: “Predicting Sector Capacity under Severe Weather Impact for Air Traffic Management”, AIAA Aviation Technology, Integration and Operations Conference, Belfast, Ireland, September, 2007.

Troxel, S.D., and C.D. Engholm: “Vertical reflectivity profiles: Averaged storm structures and applications to fan beam radar weather detection in the U.S.”, 16th Conference on Severe Local Storms, American Meteorological Society, Kananaskis Park, Alta, Canada, 1990.

Wallace, John M. and Peter V. Hobbs: Atmospheric Science – An Introductory Survey, Academic Press, Inc., 1977, pg 61.

Winfield S. Heagy, Daniel B. Kirk: “Description of URET Enhancements to Support Severe Weather Avoidance”, 4th AIAA ATIO Conference, Chicago, IL, September, 2004.

Zhang, J. K., W. Howard, C. Xia, S. Langston, S. Wang, Y. Qin: “Three-Dimensional High-Resolution National Radar Mosaic”, 11th Conference on Aviation, Range, and Aerospace Meteorology. American Meteorological Society, Hyannis, MA, October, 2004.